Journal of Computational Acoustics, Vol. 9, No. 3 (2001) 815–831

FINITE-DIFFERENCE MODELING IN MEDIA WITH MANY SMALL-SCALE CRACKS*

GERBEN B. VAN BAREN and GERARD C. HERMAN
Department of Applied Mathematics, Centre for Technical Geoscience, Delft University of Technology, Mekelweg 4, 2628 CD Delft, The Netherlands

WIM A. MULDER
Shell International Exploration and Production BV, Postbus 60, 2280AB Rijswijk, The Netherlands

Received 26 May 1999
Revised 28 February 2000

We discuss a finite-difference modeling technique for scalar, two-dimensional wave propagation in a medium containing a large number of small-scale cracks. The embedding medium can be heterogeneous. The boundaries of the cracks are not represented in the finite-difference mesh but the cracks are incorporated as distributed point sources. This enables the use of grid cells that are considerably larger than the crack sizes. We compare our method to an accurate integral-equation solution for the case of a homogeneous embedding and conclude that the finite-difference technique is accurate and computationally fast.

1. Introduction

Modeling wave propagation in media containing inclusions smaller than the wavelength of the probing wave field is of considerable interest in several areas, for instance, in seismology and in nondestructive evaluation. In seismology, variations in the subsurface of the earth are present on many scales: from scales much larger than the typical seismic wavelength down to scales that are much smaller. Heterogeneities that are much smaller than the seismic wavelength cannot be distinguished individually using seismic waves, but nevertheless can have a significant effect on the amplitude and phase of the transmitted wave field. O'Doherty and Anstey[1] demonstrated this in their classic paper for the case of plane-stratified subsurface models.

In the long-wavelength limit, a homogeneous embedding containing small-scale heterogeneities effectively behaves as a homogeneous medium, in which small-scale heterogeneities manifest themselves through apparent anisotropy and/or attenuation and dispersion. Most methods concerning wave propagation in media with embedded inclusions are based on this concept of an effective medium. An excellent overview is given by Hudson and Knopoff.[2]

*Presented at ICTCA'99, the 4th International Conference on Theoretical and Computational Acoustics, May 1999, Trieste, Italy.

Alternatively, methods have been developed that focus on the calculation of transmitted wave fields by solving a boundary-value problem. Many of these methods are limited to plane-stratified models; see, for instance, Burridge and Chang,[3] who studied pulse propagation through a one-dimensional multi-layered medium. Integral-equation methods for elastic scattering by cracks have been developed by Van der Hijden and Neerhoff[4,5]; for an overview see also Liu *et al.*[6] The case of a large number of cracks embedded in a homogeneous medium has been considered by Muijres *et al.*[7]

All methods referred to in the above are not applicable to the case of cracks in the direct vicinity of a boundary or embedded in a heterogeneous medium. Nevertheless, these situations might arise when studying, for instance, wave propagation through a cracked reservoir in a layered earth or when investigating the propagation of boundary waves in tunnel walls containing cracks. Finite-difference techniques are well-suited for solving wave propagation problems in heterogeneous media. The presence of cracks in this type of methods is accounted for by incorporating explicit boundary conditions at the crack location (see, for instance, Ref. 8). This implies that each crack boundary has to be incorporated in the finite-difference mesh, requiring a prohibitive amount of grid points in the case of a large number of small-scale cracks. In the present paper, a finite-difference technique is developed for the computation of wave propagation of scalar, two-dimensional waves in a heterogeneous medium containing a large number of small-scale cracks. Instead of imposing explicit boundary conditions at the crack boundaries, our method accounts for the presence of the cracks by introducing secondary point sources, the strength of which is computed using perturbation theory. In order to represent the point sources properly on a coarse finite-difference grid, an asymptotic method is used based on the integral representation of the scattered wave field of a small crack. The method is developed for the two-dimensional scalar case but can be extended to three dimensions and to the elastic case. These extensions are not straightforward but, nevertheless, important and we consider our method as a step in this direction.

2. Representation of the Scattered Field in Terms of Secondary Sources

We consider scalar two-dimensional wave propagation in an inhomogeneous medium containing a large number of small-scale cracks characterized by the Neumann boundary condition. In this paper, we discuss the case of a fluid medium containing rigid strips and formulate the problem in terms of the pressure. A similar formulation would describe the two-dimensional propagation of SH waves in a solid containing stress-free cracks if the pressure in our formulation is replaced by the out-of-plane displacement (propagating with the shear velocity). The velocity of the medium, c, is a function of the two-dimensional position vector, $\mathbf{x} = (x, z)$. The mth crack is denoted by D_m and its center is located at $\mathbf{x}_m = (x_m, z_m)$. This is illustrated in Fig. 1.

The unit vector normal to the crack is given by $\mathbf{n}_m = (\cos\varphi_m, \sin\varphi_m)$. The rigid crack is characterized by the Neumann boundary condition for the acoustic pressure p, given by

$$\mathbf{n}_m \cdot \nabla p(\mathbf{x}, t) = 0 \quad \mathbf{x} \in D_m \,. \tag{2.1}$$

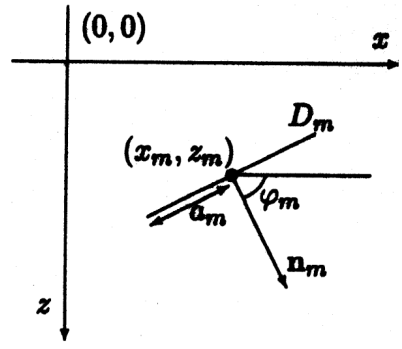

Fig. 1. Each crack is represented by a line segment D_m. It can be characterized by the position of its center, $\mathbf{x}_m = (x_m, z_m)$, its half-width a_m and the angle φ_m with the horizontal. The z-coordinate indicates depth; the x-coordinate refers to the horizontal position. The unit vector normal to the crack is defined as $\mathbf{n}_m = (\cos\varphi_m, \sin\varphi_m)$.

In the region outside the cracks, the pressure satisfies the scalar wave equation

$$(c^{-2}\partial_{tt} - \Delta)p(\mathbf{x}, t) = s(\mathbf{x}, t) \quad \mathbf{x} \notin D_m\,, \tag{2.2}$$

where ∂_{tt} is the second-order time derivative, Δ denotes the two-dimensional Laplace operator and $s(\mathbf{x}, t)$ is a source term generating the wave field. In Eq. (2.2), density variations are not taken into account for clarity of exposition. In principle, there are several ways of solving the boundary-value problem (2.1)–(2.2). For a homogeneous embedding (c constant), integral-equation methods can be used.[7] For the case of a heterogeneous embedding, however, integral-equation techniques may be impractical because they require a Green's function that is rather expensive to compute. Finite-difference techniques do not require the Green's function and are well-suited for the case of a heterogeneous embedding, but require many grid points in order to account for the explicit boundary condition (2.1) on the cracks. In the present paper, we reformulate the scattering problem in such a way that it can be incorporated in a finite-difference code without explicit modeling of the crack boundaries. This approach is especially designed for cracks that are smaller than the seismic wavelengths involved.

As a first step, the total pressure is split into the incident field p^{inc} and scattered field p^{sc}:

$$p(\mathbf{x}, t) = p^{\mathrm{inc}}(\mathbf{x}, t) + p^{\mathrm{sc}}(\mathbf{x}, t)\,. \tag{2.3}$$

By definition, the incident field satisfies the wave equation

$$(c^{-2}\partial_{tt} - \Delta)p^{\mathrm{inc}}(\mathbf{x}, t) = s(\mathbf{x}, t) \quad \mathbf{x} \in \mathbb{R}^2 \tag{2.4}$$

(without any explicit boundary conditions on the cracks). The scattered field then satisfies the source-free wave equation outside the cracks, i.e.,

$$(c^{-2}\partial_{tt} - \Delta)p^{\mathrm{sc}}(\mathbf{x}, t) = 0 \quad \mathbf{x} \notin D_m\,, \tag{2.5}$$

whereas the presence of the cracks is accounted for by the explicit boundary condition

$$\mathbf{n}_m \cdot \nabla p^{\mathrm{sc}}(\mathbf{x}, t) = -\mathbf{n}_m \cdot \nabla p^{\mathrm{inc}}(\mathbf{x}, t) \quad \mathbf{x} \in D_m\,. \tag{2.6}$$

The scattered field can be expressed in terms of field quantities at the crack locations with the aid of a boundary-integral representation.[7] This representation has the simplest form after transforming all field quantities to the frequency domain by the temporal Fourier transform. In the frequency domain, this representation has the following form:

$$\hat{p}^{\mathrm{sc}}(\mathbf{x}) = -\sum_m \int_{\mathbf{x}'\in D_m} \mathbf{n}_m \cdot \nabla \hat{p}^{\mathrm{G}}(\mathbf{x},\mathbf{x}')\hat{\phi}_m(\mathbf{x}')dS\,, \quad \mathbf{x} \notin D_m\,, \tag{2.7}$$

where $\hat{\cdot}$ denotes a Fourier-transformed quantity, $\hat{\phi}_m$ is the pressure jump across the mth crack, and $\hat{p}^{\mathrm{G}}$ denotes the Green's function of the embedding medium. For brevity, the frequency dependence of all quantities is omitted. The Green's function $\hat{p}^{\mathrm{G}}$ is defined as the solution of the Helmholtz equation for the embedding, given by:

$$(-\omega^2 c^{-2} - \Delta)\hat{p}^{\mathrm{G}}(\mathbf{x},\mathbf{x}') = \delta(\mathbf{x}-\mathbf{x}')\,, \quad \mathbf{x} \in \mathbb{R}^2\,, \tag{2.8}$$

where $\delta(\mathbf{x}-\mathbf{x}')$ denotes a point source at position $\mathbf{x}=\mathbf{x}'$.

This study is restricted to small-scale cracks, i.e., the scale of the cracks is small compared to the scale on which the wave field varies (typically smaller than 1/4 wavelength). If the cracks are small enough, we can neglect the variation of the Green's function during the integration over each crack and we can rewrite Eq. (2.7) as

$$\hat{p}^{\mathrm{sc}}(\mathbf{x}) = -\sum_m \mathbf{n}_m \cdot \nabla \hat{p}^{\mathrm{G}}(\mathbf{x},\mathbf{x_m}) \int_{\mathbf{x}'\in D_m} \hat{\phi}_m(\mathbf{x}')dS\,, \quad \mathbf{x} \notin D_m\,, \tag{2.9}$$

which implies that each crack acts as a dipole point source for the scattered field. By retaining the pressure-jump function $\hat{\phi}_m$ under the integral, we can properly account for the occurrence of singularities at the crack tips. When we compare Eq. (2.9) with Eq. (2.8), we conclude that the scattered field $\hat{p}^{\mathrm{sc}}$ can be regarded as the solution of the following equation:

$$(-\omega^2 c^{-2} - \Delta)\hat{p}^{\mathrm{sc}}(\mathbf{x}) = -\sum_m \mathbf{n}_m \cdot \nabla\delta(\mathbf{x}-\mathbf{x}_m) \int_{\mathbf{x}'\in D_m} \hat{\phi}_m(\mathbf{x}')dS\,, \quad \mathbf{x} \in \mathbb{R}^2\,, \tag{2.10}$$

where the explicit boundary conditions at the cracks are replaced by secondary point sources at the crack locations. Of course, in order to compute the secondary source strengths $\hat{\phi}_m$ at the cracks, the boundary conditions still have to be imposed. An integral-equation formulation for the source strengths can be obtained by taking the normal derivative of Eq. (2.7), choosing the point of observation close to the cracks and applying the boundary condition (2.6). However, this approach is impractical for heterogeneous media because computation of the Green's function can be very expensive. Therefore, we solve the problem by approximating the source strengths $\hat{\phi}_m$ with the aid of perturbation theory and using a finite-difference formulation for solving Eq. (2.10). Perturbation theory results in an approximate source strength

$$\int_{\mathbf{x}'\in D_m} \hat{\phi}_m(\mathbf{x}')dS \cong \pi a_m^2 \hat{q}_m\,, \tag{2.11}$$

where

$$\hat{q}_m = \mathbf{n}_m \cdot \nabla \hat{p}^{\mathrm{inc}}(\mathbf{x}_m)\,. \tag{2.12}$$

This approximation is based upon the following assumptions:

(1) Second- and higher-order scattering effects, i.e., the interactions between the different cracks, are neglected.
(2) The crack size is small compared to the wavelength of the incident wave. This implies that the incident wave is considered to be locally plane at the location of the crack and that the source strength $\hat{\phi}_m$ can be approximated by the leading-order term in a perturbation series with $\omega a_m/c$ as small parameter[9,10] (see also Ref. 7).

The first assumption is the most restrictive one in our case. In principle, it can be relaxed by taking higher-order terms into account in the Neumann-series expansion of $\hat{\phi}_m$. If we now combine Eqs. (2.10) and (2.11) and transform the resulting equation back to the time domain, we obtain the following wave equation for the scattered wave field:

$$(c^{-2}\partial_{tt} - \Delta)p^{\mathrm{sc}}(\mathbf{x},t) = -\sum_m \pi a_m^2 q_m(t)\mathbf{n}_m \cdot \nabla\delta(\mathbf{x}-\mathbf{x_m}) \quad \mathbf{x}\in\mathbb{R}^2\,, \tag{2.13}$$

with q_m the inverse Fourier transform of $\hat{q}_m$, which can be expressed in terms of the incident field by the relation

$$q_m(t) = \mathbf{n}_m \cdot \nabla p^{\mathrm{inc}}(\mathbf{x}_m,t)\,. \tag{2.14}$$

The scattering problem can be solved with the finite-difference method. First, the incident field is computed by solving Eq. (2.4) for the (heterogeneous) embedding without considering the presence of the cracks; secondly, the (first-order) scattered field is obtained by solving Eq. (2.13) with a similar technique. In this way, the problem of accounting for the explicit boundary conditions on many small cracks is avoided and replaced by the problem of accounting for the presence of many small point sources on a finite-difference grid. This is discussed in the next section. In order to find a good representation of the dipole point sources occurring on the right-hand side of Eq. (2.13), we will need a representation of the wave field in the direct vicinity of each crack. If we assume that the speed of sound in the direct vicinity of the mth crack is constant, we can express the scattered field p_m^{sc} from this single crack in the form

$$p_m^{\mathrm{sc}}(\mathbf{x},t) = -\pi a_m^2 \mathbf{n}_m \cdot \nabla \int_\rho^\infty d\tau \frac{q_m(t-\tau)}{2\pi\sqrt{\tau^2-\rho^2}} \quad (\mathbf{x}\cong\mathbf{x}_m)\,, \tag{2.15}$$

where $\rho(\mathbf{x},\mathbf{x}_m) = |\mathbf{x}-\mathbf{x}_m|/c(\mathbf{x}_m)$ is the arrival time of waves from the center of the crack $\mathbf{x}_m$ to the observation point $\mathbf{x}$. This equation is obtained by computing the inverse Fourier transform of the mth term of the summation on the right-hand side of Eq. (2.7) and using the fact that the frequency-domain Green's function $\hat{p}^{\mathrm{G}}$ for a homogeneous embedding is given by

$$\hat{p}^{\mathrm{G}}(\mathbf{x},\mathbf{x}_m) = \frac{\mathrm{i}}{4}\mathrm{H}_0^{(1)}(\omega r_m(\mathbf{x})/c(\mathbf{x}_m)) \quad (\mathbf{x}\cong\mathbf{x}_m)\,, \tag{2.16}$$

where r_m is given by

$$r_m(\mathbf{x}) = |\mathbf{x} - \mathbf{x}_m|\,, \tag{2.17}$$

and $H_0^{(1)}$ is the zeroth-order Hankel function of the first kind (see also Ref. 7). To account for the square-root singularity in Eq. (2.15), partial integration is used twice to obtain

$$p_m^{\mathrm{sc}}(\mathbf{x},t) = \frac{a_m^2}{2}\frac{\mathbf{n}_m\cdot(\mathbf{x}-\mathbf{x}_m)}{r_m^2(\mathbf{x})}\int_\rho^\infty d\tau\,\partial_{tt}q_m(t-\tau)\sqrt{\tau^2-\rho^2}\,. \tag{2.18}$$

Here we have assumed $q_m(-\infty) = 0$, because of causality. Relation (2.18) shows an important characteristic of the scattered field in a two-dimensional geometry. The whole time history of $q_m(t)$ has to be taken into account in order to calculate $p_m^{\mathrm{sc}}(\mathbf{x},t)$. Because a two-dimensional point source can be interpreted as the projection of a three-dimensional line source with infinite length, each point of the line source actually contributes to the scattered field. This could cause a problem for the finite-difference technique, since the computation of the integral is rather time-consuming. We show in the next section that this problem can be circumvented by using a series expansion for the Green's function.

3. Finite-Difference Method

In the previous section, the effect of each crack has been accounted for by the presence of a dipole point source with a strength determined by the half-width a_m and the incident field. Because point sources cannot be accurately represented in a finite difference scheme — in particular if the position of the crack does not coincide with a grid point — subgrid modeling is used. This means that the effect of each crack has to be distributed over its surrounding grid points. These grid points together should produce the same scattered field as the crack.

The discrete counterpart of the wave equation can be obtained from (2.2) by approximating the partial derivatives by finite differences and taking the quantities $p(\mathbf{x},t)$ and $s(\mathbf{x},t)$ at a grid point $\mathbf{x}_{ij}$ and discrete time t_n.

The scheme by Dablain[11] is used for the temporal discretization of the wave operator. When choosing fourth-order accuracy in time, this scheme reads

$$B^h p_{i,j}^n \equiv \frac{p_{i,j}^{n+1} - 2p_{i,j}^n + p_{i,j}^{n-1}}{(c_{i,j}\Delta t)^2} - \Delta^h p_{i,j}^n - \frac{(c_{i,j}\Delta t)^2}{12}(\Delta^h)^2 p_{i,j}^n\,. \tag{3.1}$$

Here, B^h is the discrete wave operator, being the discretization of $B = c^{-2}\partial_{tt} - \Delta$, $c_{ij} = c(\mathbf{x}_{ij})$ and Δ^h is the discretization of the Laplace operator Δ. The time-step is denoted by Δt. The second-order spatial derivative is approximated by an eighth-order scheme. For the discrete wave equation we then obtain

$$\frac{p_{i,j}^{n+1} - 2p_{i,j}^n + p_{i,j}^{n-1}}{(c_{i,j}\Delta t)^2} - \left[\Delta^h + \frac{(c_{i,j}\Delta t)^2}{12}(\Delta^h)^2\right] p_{i,j}^n = s_{i,j}^n\,. \tag{3.2}$$

In our scheme, this approach is followed both for computing the incident field p^{inc} with the aid of Eq. (2.4) and, subsequently, the scattered field p^{sc} from (2.13). In solving the latter equation, however, we have to represent a large number of dipole point sources in the finite-difference scheme. The strength of these secondary point sources can be determined by applying the (discrete) wave operator to the scattered field (2.18). The discrete version of the wave equation $Bp = s$ can be denoted by $B^h p^h = s^h$. Let $\tilde{I}^h$ be the restriction of the continuous representation of the *operator* to its discretized version. Likewise, the restriction of the continuous representation of the *solution* to the grid can be denoted by I^h. In the present case, this operator is chosen to be sampling at the grid points. If I_h defines the injection, or interpolation, from the solution on the grid to the continuous representation, then we can write $B^h = \tilde{I}^h B I_h$. A discrete source term can be obtained by letting

$$s^h = \tilde{I}^h s = \tilde{I}^h B p \simeq \tilde{I}^h B I_h I^h p = B^h I^h p \,.$$

The approximation made here is that $I_h I^h \simeq I$, meaning that the continuous solution p can be represented on the grid with sufficient accuracy. If time-step Δt and grid spacings Δx and Δz have been chosen properly with respect to the frequency content of the incident wave, this assumption is reasonable.

The discrete version of the scattered field p_m^{sc} due to the mth crack is given by $p_m^{\text{sc}}(\mathbf{x}_{i,j}, t_n)$, which is simply Eq. (2.18) evaluated at a grid points $\mathbf{x}_{i,j}$ and times t_n. Note that this representation assumes that the velocity is constant in the direct vicinity of the crack ($\mathbf{x}_{i,j} \cong \mathbf{x}_m$). The integral is computed numerically using the trapezoid rule. To obtain $q_m^h(t_n)$ at the crack, eighth-order Lagrangian interpolation and differentiation polynomials are used. Its second time-derivative $(\partial_{tt} q_m)^h(\tau)$ is computed by a fourth-order Lagrangian differentiation polynomial. If we compute (2.18) at each time and in each grid point, and substitute the resulting values in (3.2), we obtain the source distribution at each time and in each grid point:

$$s_{i,j}^n = \frac{p_m^{\text{sc}}(\mathbf{x}_{i,j}, t_{n+1}) - 2p_m^{\text{sc}}(\mathbf{x}_{i,j}, t_n) + p_m^{\text{sc}}(\mathbf{x}_{i,j}, t_{n-1})}{(c_{i,j}\Delta t)^2} - \left[\Delta^h + \frac{(\mu_{i,j}\Delta s)^2}{12}(\Delta^h)^2\right] p_m^{\text{sc}}(\mathbf{x}_{i,j}, t_n) \,. \tag{3.3}$$

Here we have used the same grid spacing in x and z, namely $\Delta s = \Delta x = \Delta z$. Furthermore, we have $\mu_{ij} = c_{ij}\Delta t / \Delta s$.

Because we are modeling a point source, we expect that the numerically constructed source distribution shows a local dominant behavior near the crack position. It therefore seems acceptable to compute the source distribution in a restricted area around the crack only. In that way, the number of points in which (2.18) has to computed can be reduced. This is supported by Fig. 2, where the numerically constructed source distribution of a horizontally oriented crack is plotted at the instant where the incident field has reached its maximum value at the crack location.

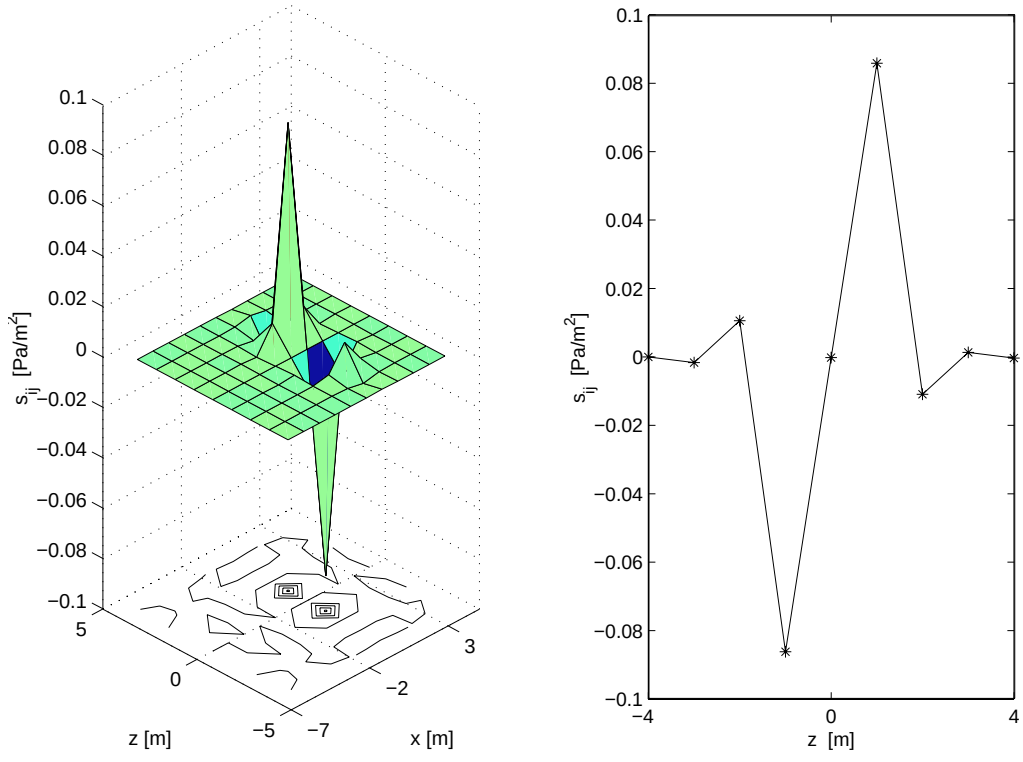

(a) (b)

Fig. 2. Numerically constructed source distribution of a horizontally oriented crack as a function of x and z (a) and a vertical cross-section through the center of the crack (b). The source values are computed by applying the discrete wave operator to the numerically computed values of the scattered pressure in the grid points.

Figure 2(a) shows the source distribution $s_{i,j}$ in the region near the crack, with a contour plot at the bottom. Figure 2(b) is a cross-section at $x = 0$. Although there are nonzero values away from the crack, it is dominated by the two peaks. Two factors influence the size of this region. If we choose it too small, information is cut off, resulting in larger errors. On the other hand, the more points we choose, the more computer memory and processing time are required. In the experiments, we have chosen this region to consist of 8×8 grid points. Outside this region, the source is assumed to be zero.

This method uses the integral representation, which is only valid for homogeneous media. Therefore the grid points involved in the area around a crack have to be in a layer with no velocity variation. In the case of multiple cracks, it does not matter if the areas of neighboring cracks overlap each other: since the wave equation is linear, different sources can be added without any problems. If two cracks are close to the same grid point, we just take the sum of the two source values at that point.

The above method for representing small cracks has some computational drawbacks. Since we use the integral representation of the scattered field, we have to store the normal

derivative of the incident field for each crack at all past times. This requires an enormous amount of memory in the case of several thousands of cracks. Furthermore, the processing time to compute (2.18) in all 64 grid points around each crack is significant.

To avoid these disadvantages, we have constructed an explicit source representation. First, we consider $\hat{B}^h\hat{p}^{\mathrm{sc}}_m(\mathbf{x},\omega)$ in the space-frequency domain and approximate it by a truncated series expansion in $k_0 r_m$ of the scattered field, where k_0 is related to the angular frequency through the relation

$$k_0 = \frac{\omega}{c(\mathbf{x}_m)}\,, \tag{3.4}$$

and r_m is given by Eq. (2.17). Finally, the results are transformed back to the space-time domain.

For the counterpart of the discrete wave operator (3.1) in space-frequency domain we obtain

$$\hat{B}^h = -k_0^2 + \frac{(\mu_{i,j}\Delta s)^2}{12}k_0^4 - \left[\Delta^h + \frac{(\mu_{i,j}\Delta s)^2}{12}(\Delta^h)^2\right], \tag{3.5}$$

which is derived in Appendix A. The space-frequency counterpart of the scattered field due to the mth crack, $\hat{p}^{\mathrm{sc}}_m$, follows from Eq. (2.15) as

$$\begin{aligned}\hat{p}^{\mathrm{sc}}_m(\mathbf{x},\omega) &= -\pi a_m^2 \mathbf{n}_m\cdot\nabla\frac{\mathrm{i}}{4}\mathrm{H}_0^{(1)}(\omega r_m(\mathbf{x})/c(\mathbf{x}_m))\hat{q}_m(\omega) \quad (\mathbf{x}\cong\mathbf{x}_m)\\ &= \pi a_m^2\frac{\mathbf{n}_m\cdot(\mathbf{x}-\mathbf{x}_m)}{r_m(\mathbf{x})}\frac{\mathrm{i}k_0}{4}H_1^{(1)}(k_0 r_m(\mathbf{x}))\hat{q}_m(\omega)\,.\end{aligned} \tag{3.6}$$

If we apply the space-frequency domain discrete wave operator to $\hat{p}^{\mathrm{sc}}_m$ of Eq. (3.6), $\hat{B}^h\hat{p}^{\mathrm{sc}}_m$ can be written as

$$\begin{aligned}\hat{B}^h\hat{p}^{\mathrm{sc}}_m(\mathbf{x},\omega) = \pi a_m^2\Bigg\{&\left(-k_0^2 + \frac{(\mu_{i,j}\Delta s)^2}{12}k_0^4 - \left[\Delta^h + \frac{(\mu_{i,j}\Delta s)^2}{12}(\Delta^h)^2\right]\right)\\ &\times\left(\frac{\mathbf{n}_m\cdot(\mathbf{x}-\mathbf{x}_m)}{r_m}\frac{\mathrm{i}k_0}{4}H_1^{(1)}(k_0 r_m)\right)\Bigg\}\hat{q}_m(\omega)\,,\\ \hat{q}_m(\omega) = \mathbf{n}_m\cdot\nabla\hat{p}^{\mathrm{inc}}(\mathbf{x}_m,\omega)\,.&\end{aligned} \tag{3.7}$$

Using the series expansion of the Hankel function up to fourth order for $k_0 r_m$ small, the part between the curly braces in (3.7) can be expressed as a polynomial in k_0 with coefficients depending only on $\mathbf{x}$ and $\mathbf{x}_m$:

$$\hat{B}^h\hat{p}^{\mathrm{sc}}_m(\mathbf{x},\omega) \cong \pi a^2\left[A_0(\mathbf{x},\mathbf{x}_m) - k_0^2 A_2(\mathbf{x},\mathbf{x}_m) + k_0^4 A_4(\mathbf{x},\mathbf{x}_m)\right]\hat{q}_m(\omega)\,, \tag{3.8}$$

where the coefficients A_0, A_2, and A_4 are given by Eqs. (B.6)–(B.8) in Appendix B.

The space-time counterpart of (3.8) is easily obtained, since the powers of k_0 are all transformed into time derivatives of $q_m(t)$. Finally, we have to combine the contributions of

all cracks and we find the following source term:

$$s(\mathbf{x},t)=\sum_m \pi a_m^2\left(A_0(\mathbf{x},\mathbf{x}_m)q_m(t)+A_2(\mathbf{x},\mathbf{x}_m)\frac{1}{c^2}\partial_{tt}q_m(t)+A_4(\mathbf{x},\mathbf{x}_m)\frac{1}{c^4}\partial_{tttt}q_m(t)\right). \tag{3.9}$$

After discretization we arrive at

$$s_{i,j}^n=\sum_m \pi a_m^2\left(A_0(\mathbf{x}_{i,j},\mathbf{x}_m)q_m^h(t_n)+A_2(\mathbf{x}_{i,j},\mathbf{x}_m)\frac{1}{c_{i,j}^2}(\partial_{tt}q_m)^h(t_n)\right.$$
$$\left.+\ A_4(\mathbf{x}_{i,j},\mathbf{x}_m)\frac{1}{c_{i,j}^4}(\partial_{tttt}q_m)^h(t_n)\right), \tag{3.10}$$

where the time derivatives can be determined by finite differences.

Because the coefficients A_0, A_2, and A_4 rapidly decrease in size with increasing distance from each crack, the source distribution can be limited to a small region around the crack. Outside this region, these coefficients are assumed to be zero. In the experiments, this region consists of 8×8 points. Because the coefficients A_0, A_2, and A_4 do not depend on time, they can be computed beforehand and stored in a grid belonging to a specific crack. The main additional computational effort involves the computation of the time derivatives of $q_m^h(t)$. The method obtained in this way, enables us to model the scattering of cracks in an efficient and accurate way. It can easily handle several thousands of cracks.

In summary, the following steps are taken in our method:

(1) Computation of the coefficients A_0, A_2, and A_4 for a given crack geometry by evaluating Eqs. (B.6)–(B.8).
(2) In each time-step, computation of the incident field p^{inc} by solving Eq. (3.2) with the seismic source represented by $s_{i,j}^n$ (no cracks). The spatial finite-difference operator Δ^h has to be the same as the one used in the computation of A_0, A_2, and A_4 (previous step).
(3) In the same time-step as mentioned under (2), computation of the scattered field p^{sc} by solving Eq. (3.2) with $s_{i,j}^n$ now given by Eq. (3.10). Again, the spatial finite-difference operator Δ^h has to be the same as the one used in the computation of A_0, A_2, and A_4.

So far, we have described only first-order scattering. The effect of multiple scattering arises in the case of more than one crack. This effect is of increasing importance when the crack size and/or the number of cracks per unit volume increases. For example, second-order scattering of a crack can be computed by taking the first-order scattered field as incident field, excluding the scattered field of that specific crack. In this way, successive terms of increasing order of the Neumann series expansion can be computed (see also Ref. 7).

In the finite-difference scheme, second-order scattering can be implemented by using the first-order scattered field in a source term for another wave equation describing the second-order scattered field. Care should be taken that the cracks do not feed on their own scattered field, that is, the scattered field of a particular crack should be removed from the scattered field that drives the source term for the same crack. However, when attempting to compute

multiple scattering, we encountered severe accuracy problems. These are partly due to the singular character of the scattered field close to the crack, and partly to the high number of derivatives of the solution that need to be taken but may not exist.

4. Validation of the Method

In order to test the validity of our finite-difference (FD) method, we compare it, for the case of a homogeneous embedding, with a boundary integral equation (BIE) method described by Muijres *et al.*[7] The BIE method is not based on the finite-difference approximation used in our method and takes into account all orders of scattering.

We consider a geometry with 3000 horizontally aligned cracks in a rectangular region of 500 m × 200 m, each crack with half-width $a_m = 1$ m. Their positions are random. The scattered wave field is computed at a receiver, located at $(x, z) = (0, 0)$. As incident field, we have taken a plane wave with a Ricker wavelet source wave form (dominant frequency: 45 Hz). The incident wave is propagating vertically downward, i.e., in a direction normal to the orientation of the cracks. The incident wave has its maximum value at $t = 0$ s and $z = 0$ m. The wave speed in the homogeneous background is $c = 2500$ m/s.

The results are shown in Fig. 3. The results are very similar. Apparently, multiple-scattering effects are negligible for this case. If the crack density increases, however, these higher-order effects can be more pronounced.

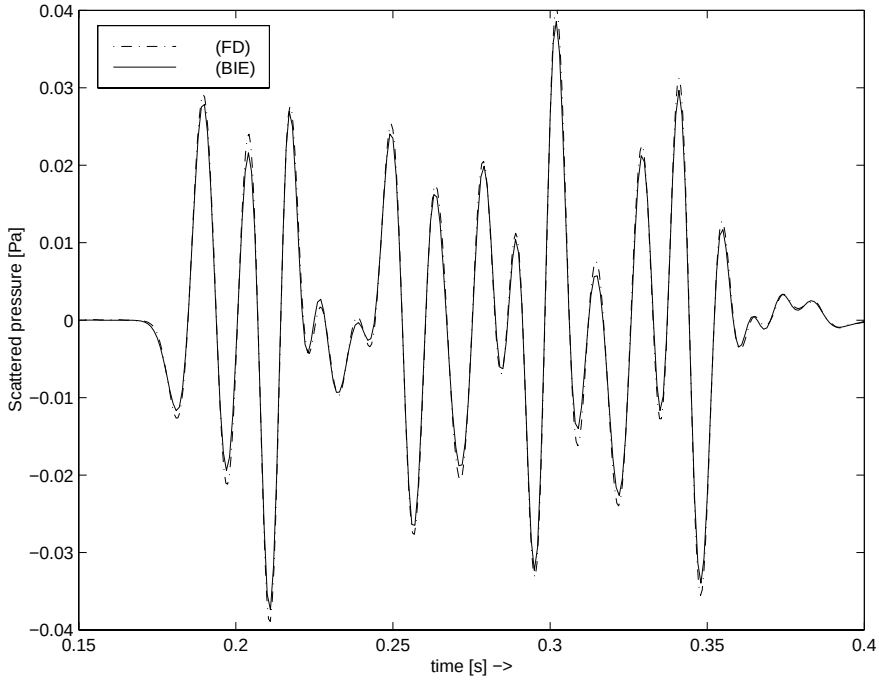

Fig. 3. Comparison of the scattered fields of the FD and BIE methods. An incident plane wave is scattered from a region with 3000 horizontally oriented cracks, embedded in a homogeneous medium with sound speed $c = 2500$ m/s.

5. Model Study for a Cross-Well Geometry

To illustrate the versatility of our method, we have simulated a cross-well experiment. We consider a low-velocity layer, containing cracks, between two high-velocity layers. The geometry is shown in Fig. 4.

A seismic source, situated in the low-velocity layer, generates the wave field; the wave field is computed at the receivers, positioned in a vertical borehole. The receivers are located at $x = 1000$ m. Their depth-coordinate ranges from $z = 1000$ m to $z = 2000$ m, the vertical spacing equals 20 m. The low-velocity layer is positioned between $z = 1300$ m and $z = 1700$ m. When the source is located in the low-velocity layer in between the two high-velocity layers, most energy emitted by the source will remain trapped in this layer as a "guided" wave. The density ρ is constant everywhere. The layer contains 4000 cracks within an area of 800 m $\times$ 300 m, centered at $(500, 1500)$. For the two coordinates of each crack, a number is generated from a uniform distribution between 0 and 1 and subsequently scaled to the proper dimensions of the model. All the cracks have the same half width a_m $(= 1$ m). We consider four cases: the case without cracks, and the cases with horizontally, vertically, and randomly oriented cracks, respectively. To generate the incident field, a point source is located in $(0, 1500)$. The source waveform is the Ricker wavelet (dominant frequency: 45 Hz).

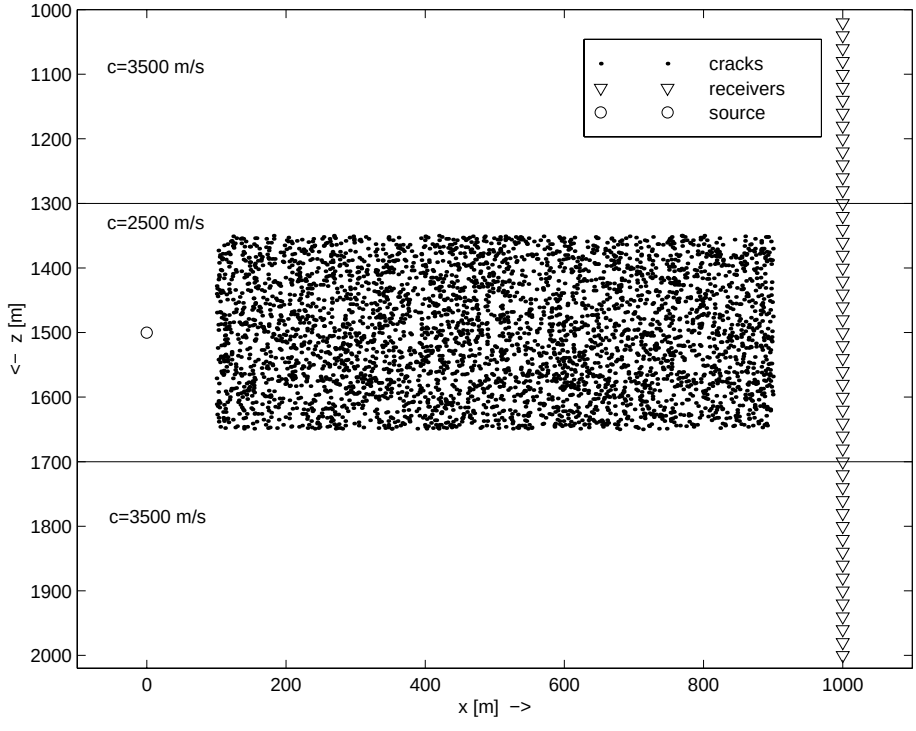

Fig. 4. Geometry of the cross-well simulation. A low-velocity layer ($c = 2500$ m/s), containing 4000 randomly positioned cracks, is embedded in two high-velocity layers ($c = 3500$ m/s). The seismic source is located in the low-velocity layer (at the left-hand side), whereas the receivers are positioned in a vertical borehole at the right.

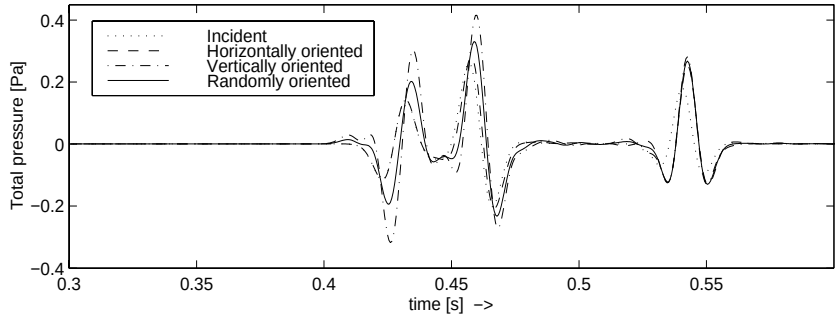

(a)

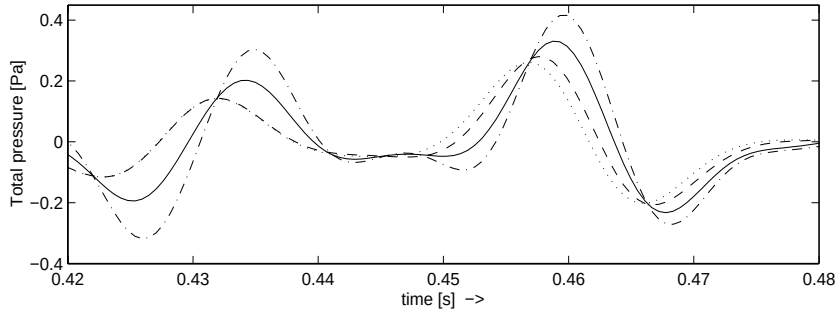

(b)

Fig. 5. Detailed comparison for a receiver at $(1000, 1500)$. Results are shown for the following cases: (i) no cracks (incident field only), (ii) all cracks horizontally aligned, (iii) all cracks vertically aligned, (iv) cracks randomly oriented. (a) Results between 0.3 s and 0.6 s, (b) Detail between 0.42 s and 0.48 s.

Figure 5 shows the results for a receiver within the layer, located at $(1000, 1500)$, for all four cases. In Fig. 5(a), we can distinguish the different arrivals of the reflections. Figure 5(b) is a detail of Fig. 5(a). It clearly shows, that the signal for the case of horizontally oriented cracks coincides with the incident field until about $t = 0.44$ s. Horizontally oriented cracks have hardly any effect on the wave field as long as it propagates parallel to the cracks. After reflection, the direction of the wave field has changed giving rise to more scattering by the horizontally oriented cracks. The cracks have the largest effect when oriented vertically; randomly oriented cracks have intermediate effects. Compared to the incident field, we observe two effects: the presence of the cracks affects the amplitudes and also results in a time delay.

6. Discussion and Conclusions

In this paper, we have presented a finite-difference method for computing the scattering of two-dimensional scalar waves by many small-scale cracks, characterized by a Neumann boundary condition. This problem arises both in the scattering of SH waves in a solid

containing stress-free cracks and in the scattering of pressure waves in a fluid containing rigid strips. As the cracks can be embedded in a heterogeneous medium, our method is an extension to methods based on integral equations which require a homogeneous background.

We have solved the problem of representing a small crack on a finite difference grid by deriving a suitable numerical source term. A further approximation of this source term provided a simpler expression that can be factored into a spatial and temporal part. This has resulted in a substantial reduction of computing time, without appreciable loss of accuracy, as became clear from the comparisons with the method of Muijres *et al.*[7] The price paid for this efficiency is a restriction to first-order scattering. Although for the given examples, multiple scattering seemed to be negligible, it might still be important if the cracks are larger or situated closer to each other. In attempting to include multiple scattering, we encountered severe accuracy problems. How to deal with multiple scattering between cracks in an efficient manner, remains to be examined.

We have considered the constant density case, but the case of varying density only results in a modified form of the wave equation (and its discretization). The derivation of the numerical source term remains the same. The extension of the present method to three spatial dimensions is possible in principle, provided the relevant perturbation expression is used for computing the secondary source strength from the incident field. In the three-dimensional case, the approximation made to simplify the source term may not be necessary, because the three-dimensional Green's function does not involve a long history in time, as in the two-dimensional case.

To simplify the analytical representations, scalar wave propagation has been studied. In principle, also the full elastic problem can be treated in a similar way. Clearly, for a realistic study of wave propagation in rocks, the elastic case should be considered. Our method is currently extended to the elastic case (although this extension is not straightforward). With the proper modifications, our method is also applicable to diffusion or potential problems.

Acknowledgements

Helpful discussions of one of the authors (GCH) with Geza Seriani in an early stage of this project are gratefully acknowledged.

Appendix A

A.1. *Derivation of the discrete wave operator in space-frequency domain*

With the scheme of Dablain,[11] as defined in Sec. 3, the discrete wave operator is given by (3.1)

$$B^h p_{i,j}^n = \frac{p_{i,j}^{n+1} - 2p_{i,j}^n + p_{i,j}^{n-1}}{(c_{ij}\Delta t)^2} - \Delta^h p_{i,j}^n - \frac{(c_{ij}\Delta t)^2}{12}(\Delta^h)^2 p_{i,j}^n \,. \tag{A.1}$$

To obtain its counterpart in space-frequency domain, we take the Fourier transform with respect to time. Furthermore, we use the relation

$$f(t-\Delta t) \overset{\mathcal{F}}{\longleftrightarrow} e^{i\omega\Delta t}\hat{f}(\omega)\,. \tag{A.2}$$

For the finite-difference approximation of the second time derivative in (A.1) we then obtain

$$\frac{p_{i,j}^{n+1}-2p_{i,j}^{n}+p_{i,j}^{n-1}}{(c_{ij}\Delta t)^2} \overset{\mathcal{F}}{\longleftrightarrow} \frac{(e^{-i\omega\Delta t}-2+e^{i\omega\Delta t})\hat{p}_{i,j}^{n}}{(c_{ij}\Delta t)^2}\,. \tag{A.3}$$

The operator in the right-hand-side of this relation can be simplified to

$$\frac{(e^{i\omega\Delta t}-2+e^{-i\omega\Delta t})}{(c_{ij}\Delta t)^2} = \frac{-4\,\sin^2\left(\dfrac{\omega\Delta t}{2}\right)}{(c_{ij}\Delta t)^2}\,. \tag{A.4}$$

If we apply a Taylor series expansion up to fourth-order of the sine function we obtain

$$\frac{-4\,\sin^2\left(\dfrac{\omega\Delta t}{2}\right)}{(c_{ij}\Delta t)^2} \cong -\frac{\omega^2}{c_{ij}^2}+\frac{1}{12}\frac{\omega^4}{c_{ij}^2}\Delta t^2 = -k_0^2+\frac{(c_{ij}\Delta t)^2}{12}k_0^4\,. \tag{A.5}$$

The spatial operator in (A.1) is not changed by the Fourier transformation and we arrive at (3.5)

$$\hat{B}^h = -k_0^2+\frac{(\mu_{ij}\Delta s)^2}{12}k_0^4-\left[\Delta^h+\frac{(\mu_{ij}\Delta s)^2}{12}(\Delta^h)^2\right]\,, \tag{A.6}$$

where $c_{ij}\Delta t$ is replaced by $\mu_{ij}\Delta s$.

Appendix B

B.1. *Approximation of the source distribution*

To find a simple expression for the source distribution of a crack, the spatial part of relation (3.7) can be expanded using a Taylor series of the Hankel function $H_1^{(1)}(k_0 r_m)$.

Observing that

$$H_1^{(1)}(w) = J_1(w) - \mathrm{i}Y_1(w)\,, \tag{B.1}$$

and using the truncated Taylor series for the Bessel functions of first and second kind,[12] we obtain

$$\begin{aligned} H_1^{(1)}(w) \cong \left\{\frac{w}{2}-\frac{w^3}{16}\right\} - i\left\{\frac{-2}{\pi w}+\left(\frac{-1+2\gamma_e-\log 4}{2\pi}\right)w+\frac{w\log w}{\pi}\right. \\ \left.+\left(\frac{\frac{5}{2}-2\gamma_e+\log 4}{16\pi}\right)w^3-\frac{w^3\log w}{8\pi}\right\}\,. \end{aligned} \tag{B.2}$$

Substitution of this expansion in (3.7), sorted into powers of k_0 and with ξ_m ($= \mathbf{n}_m \cdot (\mathbf{x} - \mathbf{x}_m)$) the coordinate along the normal of the mth crack, yields

$$\hat{B}^h(\hat{p}_m^{\mathrm{sc}}(\mathbf{x},\omega)) = \pi a_m^2 \hat{q}_m(\omega) \left(-k_0^2 + \frac{(\mu_{ij}\Delta s)^2}{12} k_0^4 - \left[\Delta^h + \frac{(\mu_{ij}\Delta s)^2}{12} (\Delta^h)^2 \right] \right)$$
$$\times \left(-\frac{\xi_m}{r_m(\mathbf{x})} k_0 \frac{i}{4} H_1^{(1)}(k_0 r_m) \right) . \tag{B.3}$$

If Δ^h is a nth-order operator, it can be shown that

$$\Delta^h \equiv \partial_{xx} + \partial_{zz} , \tag{B.4}$$

if applied to polynomials with degree less than or equal to n. For $n = 4$, this leads to a considerable simplification. Because

$$\Delta(\xi_m) = 0 ,$$
$$\Delta(\xi_m r_m^2) = 8\xi_m ,$$

both the terms containing $\log k_0$ as well as the imaginary terms vanish and what remains is expression (3.8)

$$\hat{B}^h \hat{p}_m^{\mathrm{sc}}(\mathbf{x},\omega) \cong \pi a_m^2 [A_0(\mathbf{x},\mathbf{x}_m) - k_0^2 A_2(\mathbf{x},\mathbf{x}_m) + k_0^4 A_4(\mathbf{x},\mathbf{x}_m)] \hat{q}_m(\omega) , \tag{B.5}$$

with

$$A_0(\mathbf{x},\mathbf{x}_m) = -\left[\Delta^h + \frac{(\mu_{ij}\Delta s)^2}{12} (\Delta^h)^2 \right] \frac{\mathbf{n}_m \cdot (\mathbf{x} - \mathbf{x}_m)}{2\pi r_m^2} , \tag{B.6}$$

$$A_2(\mathbf{x},\mathbf{x}_m) = \frac{\mathbf{n}_m \cdot (\mathbf{x} - \mathbf{x}_m)}{2\pi r_m^2} - \left[\Delta^h + \frac{(\mu_{ij}\Delta s)^2}{12} (\Delta^h)^2 \right] \frac{\mathbf{n}_m \cdot (\mathbf{x} - \mathbf{x}_m) \log r_m}{4\pi} , \tag{B.7}$$

$$A_4(\mathbf{x},\mathbf{x}_m) = \frac{(\mu_{ij}\Delta s)^2}{12} \frac{\mathbf{n}_m \cdot (\mathbf{x} - \mathbf{x}_m)}{2\pi r_m^2} + \frac{(3 + 4\log r_m)\mathbf{n}_m \cdot (\mathbf{x} - \mathbf{x}_m)}{16\pi}$$
$$- \left[\Delta^h + \frac{(\mu_{ij}\Delta s)^2}{12} (\Delta^h)^2 \right] \frac{\mathbf{n}_m \cdot (\mathbf{x} - \mathbf{x}_m) r_m^2 \log r_m}{32\pi} , \tag{B.8}$$

where ξ_m is replaced by $\mathbf{n}_m \cdot (\mathbf{x} - \mathbf{x}_m)$.

References

1. R. F. O'Doherty and N. A. Anstey, "Reflections on amplitudes," *Geophysical Prospecting* **19**, 430 (1971).
2. J. A. Hudson and L. Knopoff, "Predicting the overall properties of composite materials with small-scale inclusions or cracks," *PAGEOPH* **131**, 551 (1989).
3. R. Burridge and H. W. Chang, "Multimode, one-dimensional wave propagation in a highly discontinuous medium," *Wave Motion* **11**, 231 (1989).
4. J. H. M. T. Van der Hijden and F. L. Neerhoff, "Scattering of elastic waves by a plane crack of finite width," *J. Appl. Mech* **51**, 646 (1984).

5. J. H. M. T. Van der Hijden and F. L. Neerhoff, "Diffraction of elastic waves by a subsurface crack (in-plane motion)," *J. Acoust. Soc. Am.* **75**, 1694 (1984).
6. E. Liu, S. Crampin, and J. A. Hudson, "Diffraction of seismic waves by cracks with application to hydraulic fracturing," *Geophysics* **62**, 253 (1997).
7. A. J. H. Muijres, G. C. Herman, and P. G. J. Bussink, "Acoustic wave propagation in two-dimensional media containing small-scale heterogeneities," *Wave Motion* **27**, 137 (1998).
8. J. M. Carcione, "Scattering of elastic waves by single anelastic cracks and fractures," *66th Ann. Internat. Mtg., Soc. Expl. Geophys.*, expanded abstracts, 1996, pp. 654–657.
9. A. T. De Hoop, "Variational formulation of two-dimensional diffraction problems with application to diffraction by a slit," *Proc. Kon. Ned. Akad. Wet.* **B58**, 401 (1955).
10. A. T. De Hoop, "On integrals occurring in the variational formulation of diffraction problems," *Proc. Kon. Ned. Akad. Wet.* **B58**, 325 (1955).
11. M. A. Dablain, "The application of higher-order differencing to the scalar wave equation," *Geophysics* **51**, 54 (1986).
12. M. Abramowitz and I. A. Stegun, *Handbook of Mathematical Functions* (Dover Publications, 1972).